Free Radical Biology and Medicine 60 (2013) 17–28

Contents lists available at SciVerse ScienceDirect

Free Radical Biology and Medicine

journal homepage: www.elsevier.com/locate/freeradbiomed

Original contribution

Further evidence of the trypanocidal action of eupomatenoid-5: Confirmation of involvement of reactive oxygen species and mitochondria owing to a reduction in trypanothione reductase activity

D. Lazarin-Bidóia [a], V.C. Desoti [a], T. Ueda-Nakamura [a,b], B.P. Dias Filho [a,b], C.V. Nakamura [a,b], S.O. Silva [a,b,*]

[a] Programa de Pós Graduação em Ciências Farmacêuticas, Universidade Estadual de Maringá, 87020-900 Maringá, PR, Brasil
[b] Departamento de Ciências Básicas da Saúde, Universidade Estadual de Maringá, 87020-900 Maringá, PR, Brasil

ARTICLE INFO

Article history:
Received 5 November 2012
Accepted 11 January 2013
Available online 31 January 2013

Keywords:
Trypanosoma cruzi
Eupomatenoid-5
Trypanothione reductase
ROS
Mitochondria
Cell death
Free radicals

ABSTRACT

Our group assays natural products that are less toxic and more effective than available nitroheterocycles as promising therapeutic options for patients with Chagas disease. Our previous study reported the trypanocidal activity of eupomatenoid-5, a neolignan isolated from the leaves of *Piper regnellii* var. *pallescens,* against the three main parasitic forms of *Trypanosoma cruzi.* The present study further characterizes the biochemical and morphological alterations induced by this compound to elucidate the mechanisms of action involved in the cell death of *T. cruzi.* We show that eupomatenoid-5 induced oxidative imbalance in the three parasitic forms, especially trypomastigotes, reflected by a decrease in the activity of trypanothione reductase and increase in the formation of reactive oxygen species (ROS). A reduction of mitochondrial membrane potential was then triggered, further impairing the cell redox system through the production of more ROS and reactive nitrogen species. Altogether, these effects led to oxidative stress, reflected by lipid peroxidation and DNA fragmentation. These alterations are key events in the induction of parasite death through various pathways, including apoptosis, necrosis, and autophagy.

Introduction

Chagas disease, caused by the protozoan *Trypanosoma cruzi,* is considered a serious public health problem that affects approximately 10 million people in Latin America. The incidence of this disease has been estimated to include 300,000 new cases per year, and approximately 10,000 people die from this infection annually [1–3]. Since its discovery in 1909 [4], the treatment of this infection is still challenging because it is restricted to only two nitroderivative compounds, benznidazole and nifurtimox, that have limited efficacy, especially in the chronic phase of the disease, and serious side effects [5].

An urgent need exists for new active compounds that are less toxic and more effective for the treatment of patients with Chagas disease. Numerous studies have reported natural compounds with selective trypanocidal action [6]. Natural products are promising for the treatment of both infectious and noninfectious diseases because of the diversity of their molecular structures [6]. However, few studies have reported the efficacy of trypanocidal compounds against the three forms of *T. cruzi* [7,8]. The scarcity of such studies is reasonable because of the complex life cycle and distinct morphological and functional forms of *T. cruzi* [9,10]. Another important issue is that few studies have demonstrated the likely mechanisms of action of these trypanocidal compounds.

Our group recently reported the trypanocidal activity of eupomatenoid-5, a neolignan isolated from the leaves of *Piper regnellii* var. *pallescens,* against epimastigote, trypomastigote, and amastigote forms of *T. cruzi* [11–13]. This compound induced ultrastructural alterations and was shown to be more selective for parasitic cells than for mammalian cells [12,13].

Considering the trypanocidal activity of eupomatenoid-5, this study sought to better characterize the biochemical alterations induced by this compound in the three parasitic forms of *T. cruzi.* Our goal was to elucidate the mechanisms of action of eupomatenoid-5 involved in the cell death of *T. cruzi.* Based on our previous work [13], we focused our study on mitochondrial dysfunction and plasma membrane disruption induced by eupomatenoid-5. Our results provide further insights into the mechanisms of action of eupomatenoid-5 and strongly suggest that eupomatenoid-5 effectively treats Chagas disease with remarkable trypanocidal action against both forms of *T. cruzi* (i.e., trypomastigotes and amastigotes) that are relevant for mammalian infection. We suggest that the primary target for eupomatenoid-5 may be the trypanothione system, a pathway

* Corresponding author. Fax: +55 44 3011 4860.
E-mail address: lautenschlager@uem.br (S.O. Silva).

0891-5849
http://dx.doi.org/10.1016/j.freeradbiomed.2013.01.008

that is unique to the parasite and absent in the mammalian host. This system is highly dependent on trypanothione reductase (TR) and plays a key role in the antioxidant activity of trypanosomatids [14].

Materials and methods

Chemicals

Actinomycin D, antimycin A (AA), bovine serum albumin, carbonyl cyanide *m*-chlorophenylhydrazone (CCCP), digitonin, dihydrorhodamine 123 (DHR), dimethyl sulfoxide (DMSO), monodansylcadaverine (MDC), rhodamine 123 (Rh123), thiobarbituric acid, wortmannin, and 5,5′-dithiobis(2-nitrobenzoic acid) (DTNB) were purchased from Sigma–Aldrich (St. Louis, MO, USA). Dulbecco's modified Eagle's medium (DMEM) and fetal bovine serum (FBS) were obtained from Invitrogen (Grand Island, NY, USA). Annexin-V FITC, the 3,8-phenanthridinediamine-5-(6-triphenylphosphoniumhexyl)-5,6-dihydro-6-phenyl (MitoSOX) kit, propidium iodide (PI), and the terminal deoxynucleotide transferase dUTP nick-end labeling (TUNEL) kit were obtained from Invitrogen (Eugene, OR, USA). The protein assay kit was obtained from Bio-Rad (Hercules, CA, USA). All of the other reagents were of analytical grade.

Isolation of eupomatenoid-5 from leaves of P. regnellii var. pallescens

Eupomatenoid-5 (Fig. 1) was isolated from the leaves of *P. regnellii* collected in the Prof. Irenice Silva Garden of Medicinal Plants on the campus of the State University of Maringa (UEM) in Parana, Brasil. A voucher specimen (No. HUM 8392) was deposited at the UEM herbarium. The dry plant material was extracted by exhaustive maceration at room temperature in the dark in ethanol:water (90:10). Fractionation was performed from the ethyl acetate crude extract to obtain the hexane fraction, and a dihydrobenzofuran neolignan, eupomatenoid-5, was isolated from this fraction as described previously [11]. The compound was purified using absorption–chromatographic methods and identified by analyzing the ultraviolet, infrared, ^{1}H nuclear magnetic resonance (NMR), ^{13}C NMR, distortionless enhancement polarization transfer, correlated spectroscopy, heteronuclear correlation, nuclear Overhauser effect spectroscopy, heteronuclear multiple bond correlation, and gas chromatography/mass spectrometry spectra. The data were compared with the literature [15].

Stock solutions of eupomatenoid-5 were prepared aseptically in DMSO and diluted in culture medium so that the DMSO concentration did not exceed 1% in the experiments. The concentrations of eupomatenoid-5 used in the assays were based on the IC_{50} and IC_{90} values [11].

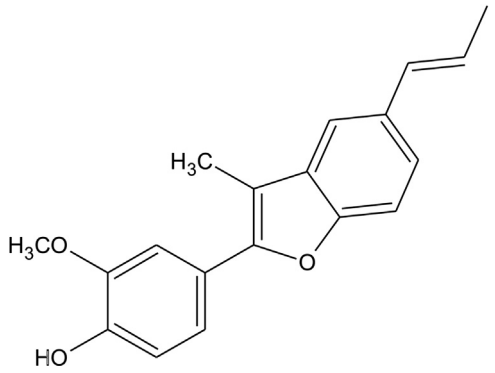

Fig. 1. Structure of eupomatenoid-5, the neolignan isolated from the leaves of *P. regnellii* var. *pallescens*.

Parasites and cell cultures

All of the experiments were performed using the Y strain of *T. cruzi*. Epimastigote forms were maintained axenically at 28 °C with weekly transfers in liver infusion tryptose medium supplemented with 10% heat-inactivated FBS at pH 7.4 [16]. Trypomastigote and amastigote forms were obtained from the supernatants of previously infected monolayers of $LLCMK_2$ cells (i.e., epithelial cells of monkey kidney (*Macaca mulatta*); CCL-7; American Type Culture Collection, Rockville, MD, USA) in DMEM supplemented with 2 mM L-glutamine, 10% FBS, and 50 mg/L gentamicin and buffered with sodium bicarbonate in a 5% CO_2 air mixture at 37 °C.

Mitochondrial membrane potential assay

Mitochondrial membrane potential ($\Delta\Psi m$) was evaluated during exposure of epimastigote forms (1×10^7 cells/ml) to 23.8, 51.0, and 170.0 μM eupomatenoid-5 for 3 h at 28 °C and exposure of trypomastigote and amastigote forms (1×10^7 cells/ml) to 34.0, 68.0, and 170.0 μM eupomatenoid-5 for 3 h at 37 °C using the fluorescent probe Rh123, which accumulates within mitochondria. Afterward, the parasites were washed and incubated with 5 μg/ml Rh123 for 15 min to verify $\Delta\Psi m$. CCCP (100.0 μM) was used as a positive control. The data acquisition and analysis were performed using a FACSCalibur flow cytometer (Becton–Dickinson, Rutherford, NJ, USA) equipped with CellQuest software (Joseph Trotter, The Scripps Research Institute, La Jolla, CA, USA). A total of 10,000 events were acquired in the region that was previously established as the one that corresponded to the parasites. Alterations in Rh123 fluorescence were quantified using an index of variation (IV) obtained from the equation $(M_T - M_C)/M_C$, in which M_T is the median fluorescence for the treated parasites and M_C is the median fluorescence for the control parasites. Negative IV values correspond to depolarization of the mitochondrial membrane.

Cell membrane integrity assay

Cell membrane integrity was evaluated during exposure of epimastigote forms (1×10^7 cells/ml) to 23.8, 51.0, and 170.0 μM eupomatenoid-5 for 3 h at 28 °C and exposure of trypomastigote and amastigote forms (1×10^7 cells/ml) to 34.0, 68.0, and 170.0 μM eupomatenoid-5 for 3 h at 37 °C using PI, a probe that binds to DNA in ruptured membrane cells. Afterward, the parasites were washed and incubated with 0.2 μg/ml PI for 10 min to verify cell membrane integrity. Digitonin (40.0 μM) was used as a positive control. Data acquisition and analysis were performed using a FACSCalibur flow cytometer equipped with CellQuest software. A total of 10,000 events were acquired in the region that was previously established as the one that corresponded to the parasites. Alterations in the fluorescence of PI were quantified as the percentage of increase in the fluorescence compared with the control (untreated parasites).

Fluorimetric detection of mitochondrial-derived superoxide anion ($O_2^{\bullet -}$)

The mitochondrial production of $O_2^{\bullet -}$ was evaluated during exposure of epimastigote forms to 23.8, 51.0, and 170.0 μM eupomatenoid-5 and exposure of trypomastigote and amastigote forms to 34.0, 68.0, and 170.0 μM eupomatenoid-5 using the fluorescent $O_2^{\bullet -}$-sensitive, mitochondrial-targeted probe MitoSOX.

Parasites (2×10^7 cells/ml) were loaded with 5 μM MitoSOX for 10 min at 22 °C and then washed with Krebs–Henseleit (KH) buffer (pH 7.3) that contained 15 mM $NaHCO_3$, 5 mM KCl, 120 mM NaCl, 0.7 mM Na_2HPO_4, and 1.5 mM NaH_2PO_4. Loaded cells were exposed to the stimuli, and after suitable times fluorescence was measured in a fluorescence microplate reader (Victor X3; PerkinElmer) at $\lambda_{ex}=510$ nm and $\lambda_{em}=580$ nm. Oxidized MitoSOX becomes highly fluorescent upon binding to nucleic acids. Cells were exposed to 10 μM AA, a stimulus known to induce mitochondrial $O_2^{\bullet -}$ production.

Fluorimetric detection of oxidant species production

The production of oxidant species (reactive oxygen and nitrogen species (ROS/RNS)) was evaluated during exposure of epimastigote forms to 23.8, 51.0, and 170.0 μM eupomatenoid-5 and exposure of trypomastigote and amastigote forms to 34.0, 68.0, and 170.0 μM eupomatenoid-5 using the nonfluorescent probe DHR by measuring its oxidation to the fluorescent product Rh123 [17]. Parasites (2×10^7 cells/ml) were loaded with 50 μM DHR for 30 min at 37 °C and washed with KH buffer (pH 7.3) to eliminate unincorporated probe. Loaded cells were exposed to the stimuli, and after suitable times Rh123 fluorescence was determined in a fluorescence microplate reader (Victor X3; PerkinElmer) at $\lambda_{ex}=485$ nm and $\lambda_{em}=520$ nm. AA (10 μM) was used as a positive control.

Estimation of decrease in reduced thiol level

In the trypanothione system, trypanothione is reduced to a dithiol $T(SH)_2$ by TR. The inhibition of TR decreases total reduced thiol [18]. Free thiol levels were determined using DTNB. Epimastigote forms were treated with 23.8, 51.0, and 170.0 μM eupomatenoid-5 for 3, 24, and 96 h at 28 °C. Trypomastigote and amastigote forms were treated with 34.0, 68.0, and 170.0 μM eupomatenoid-5 for 3 and 24 h at 37 °C. Afterward, the cells (1×10^7 cells/ml) were centrifuged, dissolved in 10 mM Tris–HCl buffer (pH 2.5), and sonicated. Acidic pH was used during sonication to prevent oxidation of the free thiol groups. Cellular debris was removed by centrifugation, and 100 μl of the supernatant and 100 μl of 500 mM phosphate buffer (pH 7.5) were placed in each microtiter well, followed by the addition of 20 μl of 1 mM DTNB to each well. Absorbance was measured at 412 nm.

Lipid peroxidation assay

The extent of lipid peroxidation was determined as the amount of thiobarbituric acid-reactive substances (TBARS) in terms of malondialdehyde (MDA). Epimastigote forms (12 mg/ml) were treated with 23.8, 51.0, and 170.0 μM eupomatenoid-5 for 3 h at 28 °C. Trypomastigote and amastigote forms (12 mg/ml) were treated with 34.0, 68.0, and 170.0 μM eupomatenoid-5 for 3 h at 37 °C. After incubation, the samples (0.5 mg protein) were heated in a solution that contained 0.37% thiobarbituric acid, 15% trichloroacetic acid, and 0.25 N HCl for 45 min at 95 °C. After cooling, absorbance was read at 532 nm, and the TBARS concentration was calculated based on an ε value of 153,000 M^{-1} cm^{-1} [19].

DNA fragmentation

DNA double-strand ruptures were evaluated in situ using TUNEL. Epimastigote forms (1×10^7 cells/ml) were treated with 23.8, 51.0, and 170.0 μM eupomatenoid-5 for 24 h at 28 °C. Trypomastigote and amastigote forms (1×10^7 cells/ml) were treated with 34.0, 68.0, and 170.0 μM eupomatenoid-5 for 24 h at 37 °C. Afterward, the cells were fixed and subjected to the TUNEL assay according to the manufacturer's instructions. Actinomycin D (10.0 μg/ml) was used as a positive control. The nuclei were counterstained with PI, which denotes the condensation and margination of chromatin. Cells that undergo DNA double-strand ruptures should fluoresce brightly when viewed with appropriate filter sets, unlike the untreated cells. Fluorescence was observed under an Olympus BX51 fluorescence microscope, and pictures were captured using an Olympus UC30 camera.

Phosphatidylserine exposure

Phosphatidylserine exposure was detected using annexin-V FITC, a calcium-dependent phospholipid binding protein. Epimastigote forms (1×10^7 cells/ml) were treated with 23.8, 51.0, and 170.0 μM eupomatenoid-5 for 3 h at 28 °C. Trypomastigote and amastigote forms (1×10^7 cells/ml) were treated with 34.0, 68.0, and 170.0 μM eupomatenoid-5 for 3 h at 37 °C. Afterward, the cells were washed and resuspended in 100 μl of binding buffer (140 mM NaCl, 5 mM $CaCl_2$, and 10 mM Hepes–Na, pH 7.4), followed by the addition of 5 μl annexin-V FITC for 15 min at room temperature. Binding buffer (400 μl) and 50 μl PI were then added. AA (125.0 μM) was used as a positive control. Data acquisition and analysis were performed using a FACSCalibur flow cytometer equipped with CellQuest software. A total of 10,000 events were acquired in the region that was previously established as the one that corresponded to the parasites. Cells that were stained with annexin-V (PI positive or negative) were considered apoptotic, and cells that were only PI positive were considered necrotic [20].

Cell volume determination

Epimastigote forms (1×10^7 cells/ml) treated with 23.8, 51.0, and 170.0 μM eupomatenoid-5 for 3 h at 28 °C and trypomastigote and amastigote forms (1×10^7 cells/ml) treated with 34.0, 68.0, and 170.0 μM eupomatenoid-5 for 3 h at 37 °C were collected by centrifugation, washed twice in phosphate-buffered saline (PBS), resuspended in PBS, and analyzed using fluorescence-activated cell sorting and a FACSCalibur flow cytometer. Actinomycin D (20.0 mM) was used as a positive control. A total of 10,000 events were acquired in the region that was previously established as the one that corresponded to the parasites. Histograms were generated, and the analysis was performed using CellQuest software; forward light scatter (FSC-H) represents the cell volume.

Evaluation of autophagic vacuoles

Autophagic vacuoles were evaluated using labeling with MDC, a fluorescent probe that accumulates in autophagic vacuoles [21,22]. Epimastigote forms (1×10^7 cells/ml) were treated with 23.8, 51.0, and 170.0 μM eupomatenoid-5 for 24 h at 28 °C, and trypomastigote and amastigote forms (1×10^7 cells/ml) were treated with 34.0, 68.0, and 170.0 μM eupomatenoid-5 for 24 h at 37 °C. The cells were then incubated with 0.05 mM MDC in PBS for 15 min. After incubation, the cells were washed twice in PBS. MDC stain was analyzed using an Olympus BX51 fluorescence microscope, and images were captured using a UC30 camera. In some of the experiments, before the induction of autophagy, the cells were pretreated with wortmannin, a potent inhibitor of PI3 kinase, an enzyme associated with the signaling pathway involved in the regulation of autophagy [23].

Statistical analysis

The data shown in the graphs are expressed as the means ± standard error of the mean of independent preparations. The data were analyzed using one- and two-way analysis of variance. Significant differences among means were identified using the Tukey post hoc test. Values of $p \leq 0.05$ were considered statistically significant. Statistical analyses were performed using the Statistica software package.

Results

Effect of eupomatenoid-5 on the mitochondrial membrane potential of T. cruzi

A previous electron microscopy study showed the effect of eupomatenoid-5 on *T. cruzi* mitochondria [12]. Based on this, we decided to evaluate the ΔΨm in eupomatenoid-5-treated parasites. The histograms showed a marked decrease in total Rh123 fluorescence intensity in the three parasitic forms after 3 h treatment, indicating mitochondrial depolarization (Fig. 2, Table 1). This loss of ΔΨm was dose-dependent and significantly different for the three parasitic forms at all of the concentrations tested compared with the control group. However, the loss of ΔΨm was noticeably more pronounced in trypomastigote and amastigote forms, in which ΔΨm reductions greater than 70.0% were observed at all of the concentrations tested. Additionally, a drop of over 90% in fluorescence intensity was observed with the higher concentration of eupomatenoid-5 (170.0 μM) for the three parasitic forms. The positive control, CCCP, in epimastigotes, trypomastigotes, and amastigotes induced 82.2, 84.6, and 84.7% changes in mitochondrial membrane potential, respectively.

Effect of eupomatenoid-5 on cell membrane integrity of T. cruzi

Our previous work also demonstrated that eupomatenoid-5 induced cell membrane disruption [13]. This prompted us to evaluate cell membrane integrity in eupomatenoid-5-treated parasites. Eupomatenoid-5 affected the membrane integrity of epimastigotes, trypomastigotes, and amastigotes of *T. cruzi* compared with untreated cells (Fig. 3). The histograms showed an increase in the intensity of PI fluorescence (33–83% PI-positive parasites), mainly for trypomastigotes, at all of the concentrations tested, indicating alterations in cell membrane integrity. For epimastigotes, at higher concentrations, approximately 60% of the parasites were PI positive. For amastigotes, even at the higher concentration, only 35% of the parasites were PI positive. The positive control, digitonin, in epimastigotes, trypomastigotes, and amastigotes increased fluorescence by 99.04, 55.45, and 98.70%, respectively.

Effect of eupomatenoid-5 on mitochondrial-derived $O_2^{\bullet -}$ production in T. cruzi

Changes in ΔΨm can induce numerous mitochondrial disorders that seriously compromise mitochondrial function and consequently cell viability. A classic example of a disorder induced by ΔΨm alterations is an increase in the production of ROS through the electron transport chain [24]. Thus, based on our ΔΨm results, we evaluated $O_2^{\bullet -}$ production in eupomatenoid-5-treated parasites. Fig. 4 shows a significant increase in the production of mitochondrial $O_2^{\bullet -}$ at all of the concentrations and times tested for the three parasitic forms compared with the control group. Eupomatenoid-5 induced a pronounced effect on trypomastigote forms, with up to threefold increases in $O_2^{\bullet -}$ production after 3 h (Fig. 4B). Epimastigotes were somewhat

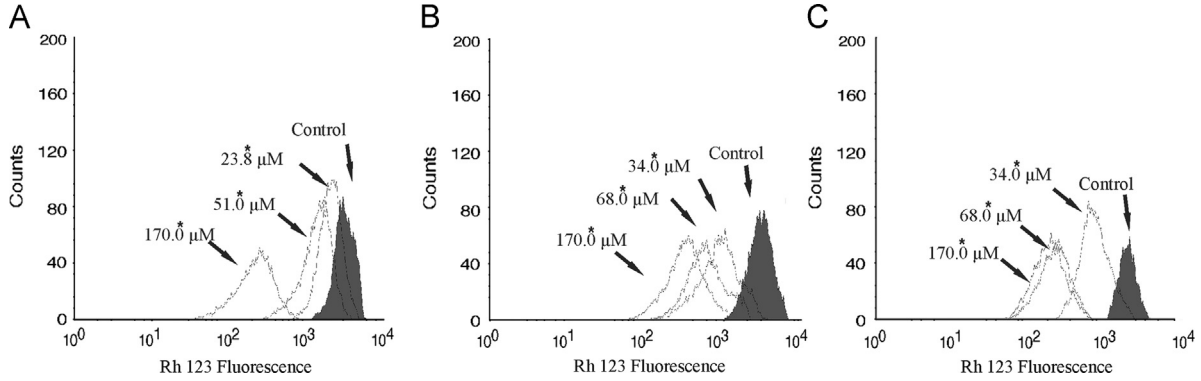

Fig. 2. Mitochondrial membrane potential assay in parasitic forms of *T. cruzi* treated with eupomatenoid-5 for 3 h and stained with Rh123, which accumulates within mitochondria. (A) Epimastigotes treated with 23.8, 51.0, and 170.0 μM. (B) Trypomastigotes treated with 34.0, 68.0, and 170.0 μM. (C) Amastigotes treated with 34.0, 68.0, and 170.0 μM. Arrows correspond to concentrations tested. Control group (untreated cells) is also shown. Typical histograms of at least three independent experiments are depicted. *$p \leq 0.05$, significant difference relative to the control group (untreated cells).

Table 1
Mitochondrial membrane potential assay in parasitic forms of *Trypanosoma cruzi* treated with eupomatenoid-5 for 3 h and stained with Rh123.

Epimastigotes			Trypomastigotes			Amastigotes		
μM	Median	IV[a]	μM	Median	IV[a]	μM	Median	IV[a]
Control	3078.09	0.0	Control	2942.73	0.0	Control	2308.24	0.0
23.8	2072.08*	−0.3	34.0	889.65*	−0.7	34.0	820.47*	−0.7
51.0	1420.18*	−0.5	68.0	577.72*	−0.8	68.0	248.05*	−0.9
170.0	226.71*	−0.9	170.0	321.97*	−0.9	170.0	207.21*	−0.9

[a] $IV = (M_T - M_C)/M_C$, where M_T corresponds to the median of the fluorescence for treated parasites and M_C to that for control parasites.
* $p \leq 0.05$, significant difference relative to the control group (untreated cells).

more sensitive to the production of mitochondrial $O_2^{\bullet -}$ than were amastigotes. The positive control, AA, also induced two-, three-, and onefold increases in mitochondrial $O_2^{\bullet -}$ production in epimastigotes, trypomastigotes, and amastigotes, respectively.

Effect of eupomatenoid-5 on oxidant species production in T. cruzi

Based on the MitoSOX data, we evaluated the effects of total ROS/RNS production in eupomatenoid-5-treated parasites. A significant dose-dependent increase in Rh123 fluorescence was observed at all of the concentrations tested for the three parasitic forms after 1 and 2 h treatment compared with the control group (Fig. 5). Remarkably, with 3 h eupomatenoid-5 treatment, we observed a significant decrease in Rh123 fluorescence at all of the concentrations tested for the three parasitic forms compared with 1 and 2 h treatment. This signal loss at 3 h may indicate membrane depolarization, which is consistent with our previous $\Delta\Psi m$ data. The increase in ROS/RNS production was somewhat higher in trypomastigotes (80–150% of Rh123 fluorescence) than in epimastigotes and amastigotes (50–110% of Rh123 fluorescence). The positive control, AA, induced an increase of 50% in Rh123 fluorescence in epimastigotes, trypomastigotes, and amastigotes, even with 1 h incubation.

Effect of eupomatenoid-5 on reduced thiol levels of T. cruzi

Our data suggested that eupomatenoid-5 is an inducer of oxidative imbalance, attributable to enhanced ROS/RNS production. Because conditions of oxidative imbalance depend on both increased oxidant species and decreased antioxidant effectiveness [25], our next step was to assess the activity of TR. A significant dose-dependent decrease in total reduced thiol levels was observed at all of the concentrations and times tested for all three parasitic forms compared with the control group, with the exception of epimastigotes treated with 23.8 μM eupomatenoid-5 for 3 h (Fig. 6). Trypomastigotes were the most sensitive to the action of eupomatenoid-5, exhibiting around 30 and 40% decreases in total reduced thiol levels after 3 and 24 h treatment, respectively.

Effect of eupomatenoid-5 on lipid peroxidation of T. cruzi

Our previous experiment demonstrated that eupomatenoid-5 induced oxidative imbalance in *T. cruzi*, leading to enhanced ROS/RNS production and impaired antioxidant defense. Based on this we expected that eupomatenoid-5 may trigger molecular and structural alterations in the parasite through oxidative reactions. Strong evidence of this was provided by the plasma membrane disruption results described above. To confirm this, we measured TBARS production, which is frequently used to quantify lipoperoxidation of the cell membrane, in eupomatenoid-5-treated parasites [26]. Fig. 7 shows that the increase in MDA in the three parasitic forms was significantly different after 3 h compared with the control group. This increase was dose-dependent and more pronounced for trypomastigotes (up to 4.3-fold), followed by epimastigotes (up to 3.3-fold) and amastigotes (up to 2.7-fold).

Effect of eupomatenoid-5 on DNA fragmentation of T. cruzi

The oxidative imbalance induced by eupomatenoid-5 might also trigger destructive effects on DNA [27]. As shown in Fig. 8,

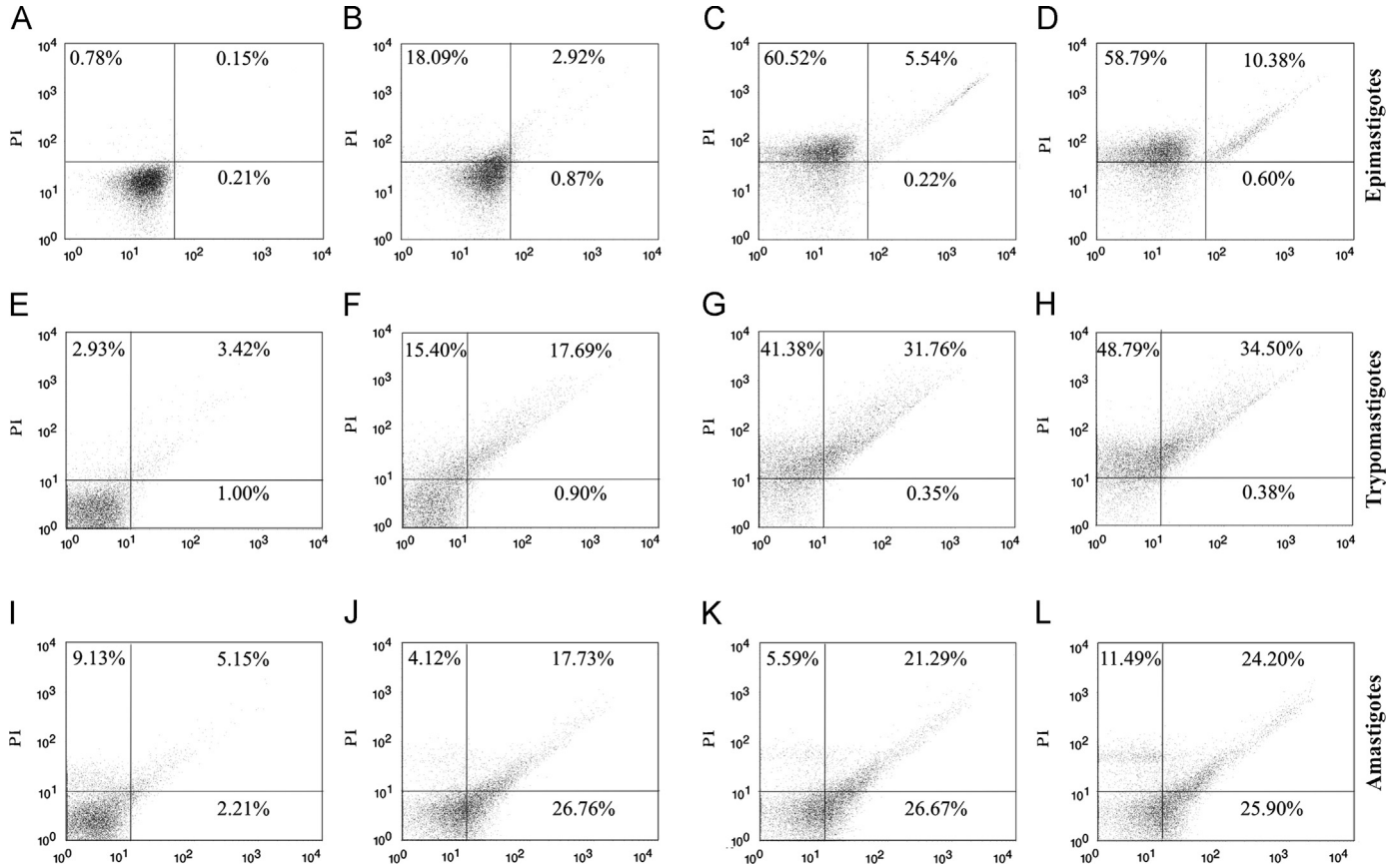

Fig. 3. Cell membrane integrity assay in parasitic forms of *T. cruzi* treated with eupomatenoid-5 for 3 h and stained with PI, a probe that binds to DNA in ruptured membrane cells. (A) Untreated epimastigotes. (B, C, D) Epimastigotes treated with 23.8, 51.0, and 170.0 μM. (E) Untreated trypomastigotes. (F, G, H) Trypomastigotes treated with 34.0, 68.0, and 170.0 μM. (I) Untreated amastigotes. (J, K, L) amastigotes treated with 34.0, 68.0, and 170.0 μM. Percentage of PI-stained positive cells is shown in the upper right and left quadrants. Typical histograms of at least three independent experiments are depicted.

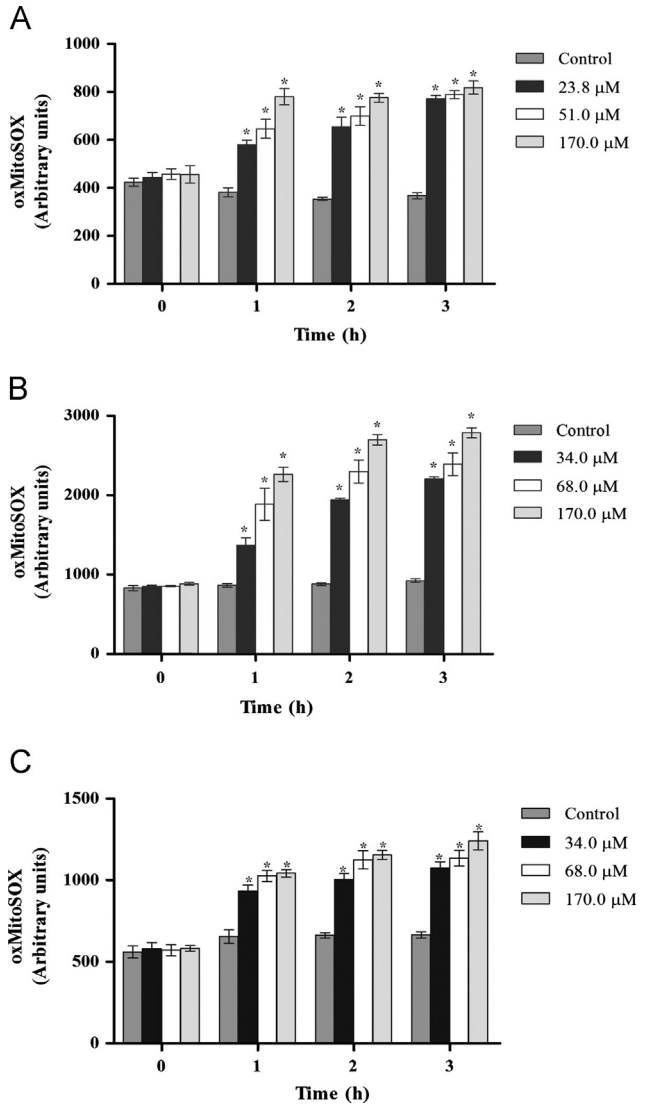

Fig. 4. Mitochondrial $O_2^{\bullet -}$ production in parasitic forms of *T. cruzi* treated with eupomatenoid-5 for up to 3 h using the fluorescent probe MitoSOX. Parasites preloaded with MitoSOX were incubated with various concentrations of eupomatenoid-5. (A) Epimastigotes treated with 23.8, 51.0, and 170.0 μM. (B) Trypomastigotes treated with 34.0, 68.0, and 170.0 μM. (C) Amastigotes treated with 34.0, 68.0, and 170.0 μM. At the indicated times parasites were used to fluorimetrically measure oxidized MitoSOX (oxMitoSOX). Results are expressed as mean fluorescence (in arbitrary units) ± SD of at least three independent experiments. $^*p \leq 0.05$, significant difference relative to the control group (untreated cells).

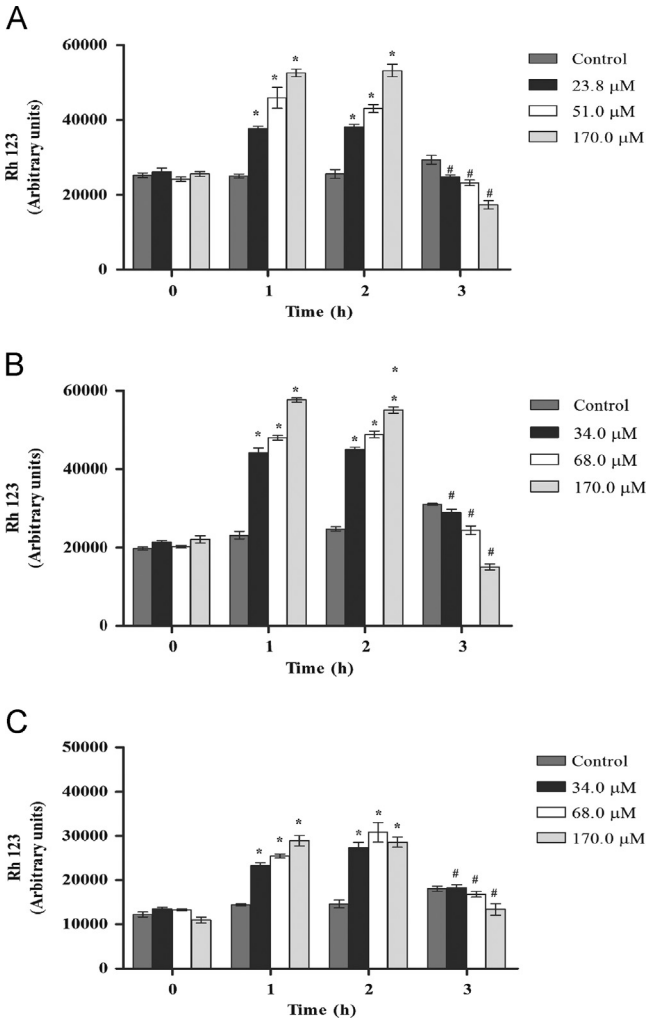

Fig. 5. Production of ROS/RNS in parasitic forms of *T. cruzi* treated with eupomatenoid-5 for up to 3 h using the nonfluorescent probe DHR. Parasites preloaded with DHR were incubated with various concentrations of eupomatenoid-5 and Rh123 fluorescence was measured. (A) Epimastigotes treated with 23.8, 51.0, and 170.0 μM. (B) Trypomastigotes treated with 34.0, 68.0, and 170.0 μM. (C) Amastigotes treated with 34.0, 68.0, and 170.0 μM. Results are expressed as mean fluorescence (in arbitrary units) ± SD of at least three independent experiments. $^*p \leq 0.05$, treated vs control group; $\#p \leq 0.05$, treated for 3 h vs treated for 1 and 2 h.

the three parasitic forms treated with various concentrations of eupomatenoid-5 and subjected to the TUNEL assay exhibited bright fluorescence, indicating DNA fragmentation compared with untreated parasites. Additionally, counterstaining with PI in epimastigotes, trypomastigotes, and amastigotes revealed that eupomatenoid-5 induced chromatin condensation and margination [28]. Bright fluorescence was also observed with actinomycin D, a known inducer of apoptosis (data not shown).

Effect of eupomatenoid-5 on phosphatidylserine exposure in T. cruzi

The effect of eupomatenoid-5 on DNA prompted us to explore the action of this compound on the apoptosis cell death pathway. Apoptosis is characterized by several biochemical alterations, including DNA fragmentation and phosphatidylserine exposure [29]. Therefore, we evaluated whether eupomatenoid-5 induces phosphatidylserine exposure. As shown in Fig. 9, the three parasitic forms treated with various concentrations of eupomatenoid-5 exhibited an increase in annexin-V fluorescence intensity, indicating phosphatidylserine exposure, compared with the untreated parasites. The histograms showed an increase of 34–56% in the intensity of annexin-V fluorescence at all of the concentrations tested for trypomastigotes. For epimastigotes, at the higher concentration, annexin-V fluorescence was observed in approximately 65% of the parasites. For amastigotes, even at the higher concentration, annexin-V fluorescence was observed in only 43% of the parasites.

Effect of eupomatenoid-5 on cell volume of T. cruzi

In addition to biochemical alterations, apoptosis also induces morphological alterations. Based on this, we performed additional experiments to evaluate cell shrinkage, also a hallmark of apoptotic death, in eupomatenoid-5-treated parasites [29]. As shown in Fig. 10, a significant decrease in cell volume was observed at all of the concentrations tested for the three parasitic forms compared with the control group. Additionally, trypomastigotes were more sensitive to the effect of eupomatenoid-5, exhibiting

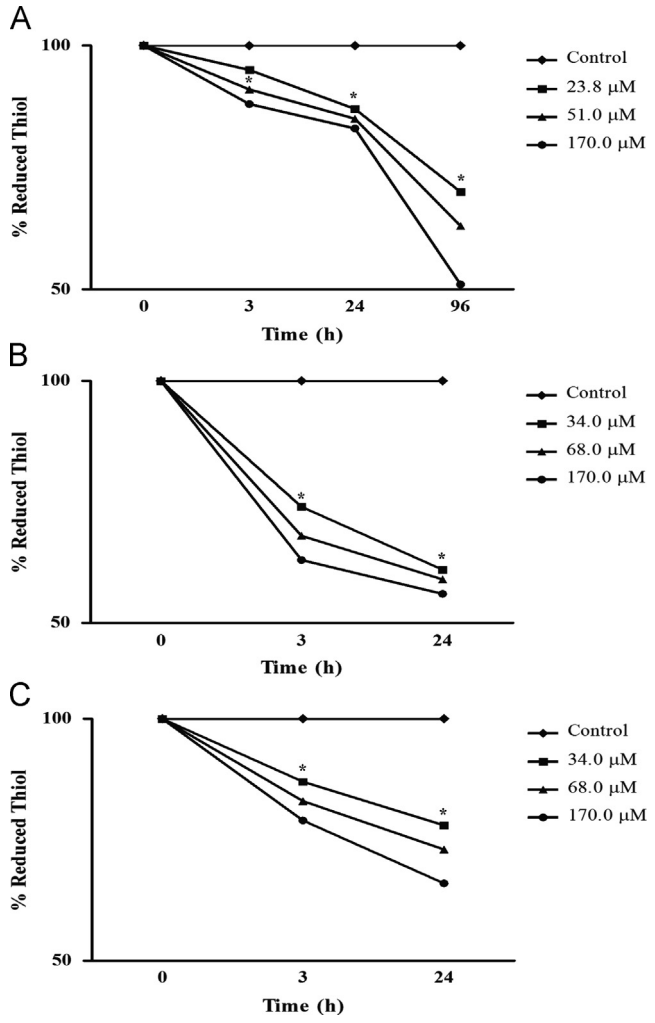

Fig. 6. Thiol levels in parasitic forms of *T. cruzi* treated with eupomatenoid-5 using DTNB. (A) Epimastigotes treated with 23.8, 51.0, and 170.0 μM for 3, 24, and 96 h. (B) Trypomastigotes treated with 34.0, 68.0, and 170.0 μM for 3 and 24 h. (C) Amastigotes treated with 34.0, 68.0, and 170.0 μM for 3 and 24 h. The results are expressed as mean ± SD of at least three independent experiments. $^{*}p \leq 0.05$, significant difference relative to the control group (untreated cells).

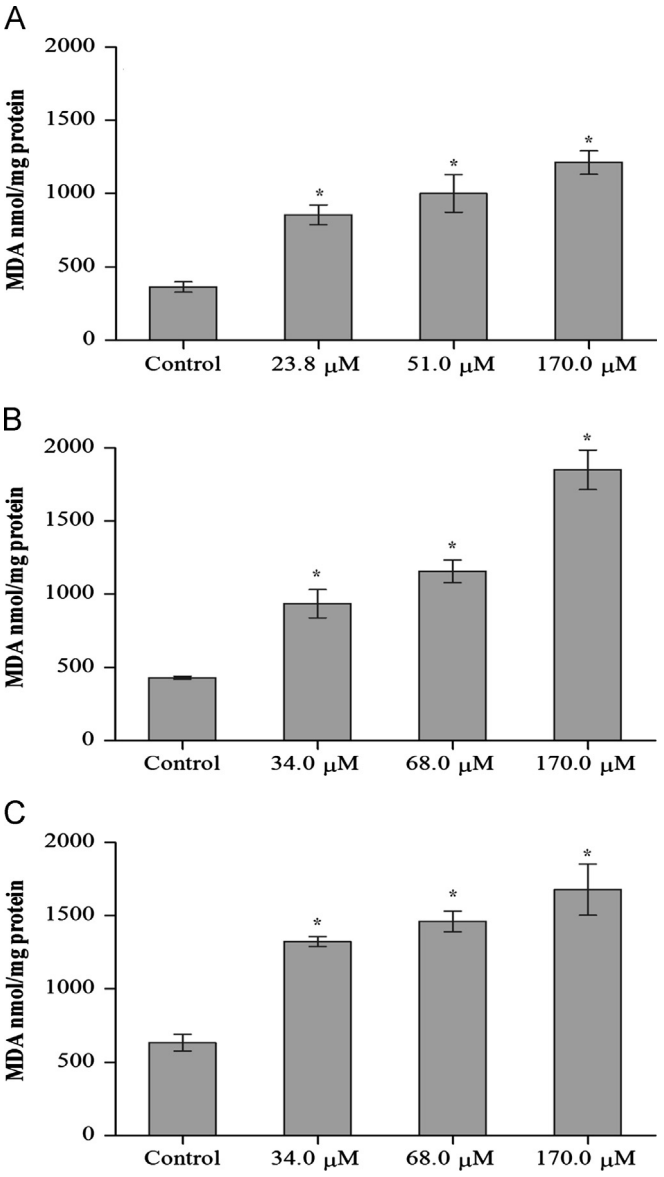

Fig. 7. Lipid peroxidation in parasitic forms of *T. cruzi* treated with eupomatenoid-5 for 3 h determined as the amount of TBARS in terms of MDA. (A) Epimastigotes treated with 23.8, 51.0, and 170.0 μM. (B) Trypomastigotes treated with 34.0, 68.0, and 170.0 μM. (C) Amastigotes treated with 34.0, 68.0, and 170.0 μM. The results are expressed as mean ± SD of at least three independent experiments. $^{*}p \leq 0.05$, significant difference relative to the control group (untreated cells).

a decrease in cell volume of greater than 80.0% at all of the concentrations tested (Fig. 10B). The effect of eupomatenoid-5 was less in epimastigotes and amastigotes than in trypomastigotes. The positive control, actinomycin D, in epimastigotes, trypomastigotes, and amastigotes decreased cell volumes by 28, 71, and 41%, respectively.

Effect of eupomatenoid-5 on the formation of autophagic vacuoles in T. cruzi

Based on our previous transmission electron microscopy study [12], which found abnormalities that suggested autophagosomes on *T. cruzi* treated with eupomatenoid-5, we evaluated whether autophagy is an alternative pathway of cell death induced by eupomatenoid-5. Fig. 11 shows the presence of fluorescence in rounded structures in the three parasitic forms, indicating the formation of autophagic vacuoles compared with untreated parasites. This effect could be partially prevented in the parasites pretreated with wortmannin.

Discussion

Numerous natural and synthetic compounds [6,30] have been studied over the past 100 years for the treatment of Chagas disease since its discovery in 1909 [4]. Nevertheless, the treatment of this infection remains a problem, especially in the chronic phase of the disease when amastigotes are the predominant form. Our previous studies demonstrated the effective and selective action of eupomatenoid-5 against the main forms of *T. cruzi*. Additionally, eupomatenoid-5 was shown to induce important ultrastructural alterations in the three forms of *T. cruzi*, revealed by electronic microscopy [12,13]. In this context, the present study sought to further elucidate the mechanism of action of eupomatenoid-5 in the cell death of this protozoan.

We initially focused our studies on investigating alterations in mitochondria and the plasma membrane by staining the parasites with Rh123 and PI. Considering the high sensitivity of these

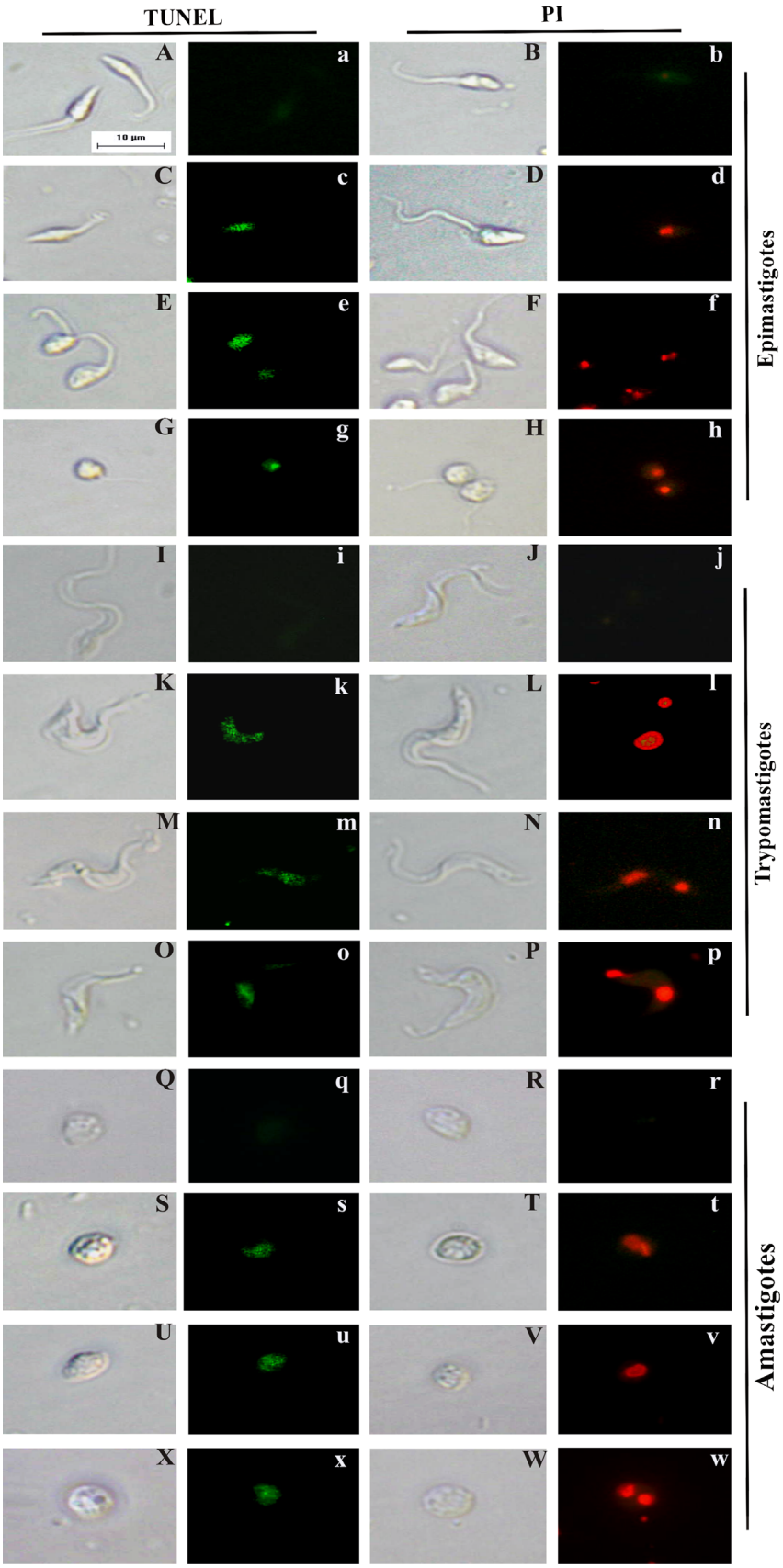

Fig. 8. DNA fragmentation in parasitic forms of *T. cruzi* treated with eupomatenoid-5 for 24 h using TUNEL assay. (A–X) Differential interference contrast (DIC). (a–x) Fluorescence images of TUNEL and PI assays. (A, a, B, b) Untreated epimastigotes. (C, c, E, e, G, g) Epimastigotes treated with 23.8, 51.0, and 170.0 µM. (D, d, F, f, H, h) Epimastigotes treated with 23.8, 51.0, and 170.0 µM and counterstaining with PI. (I, i, J, j) Untreated trypomastigotes. (K, k, M, m, O, o) Trypomastigotes treated with 34.0, 68.0, and 170.0 µM. (L, l, N, n, P, p) Trypomastigotes treated with 34.0, 68.0, and 170.0 µM and counterstaining with PI. (Q, q, R, r) Untreated amastigotes. (S, s, U, u, X, x) Amastigotes treated with 34.0, 68.0, and 170.0 µM. (T, t, V, v, W, w) Amastigotes treated with 34.0, 68.0, and 170.0 µM and counterstaining with PI. Green fluorescence indicates DNA fragmentation and red fluorescence indicates condensation and margination of chromatin. The images are representative of treated epimastigotes, trypomastigotes, and amastigotes of at least three independent experiments. Scale bar, 10 µm.

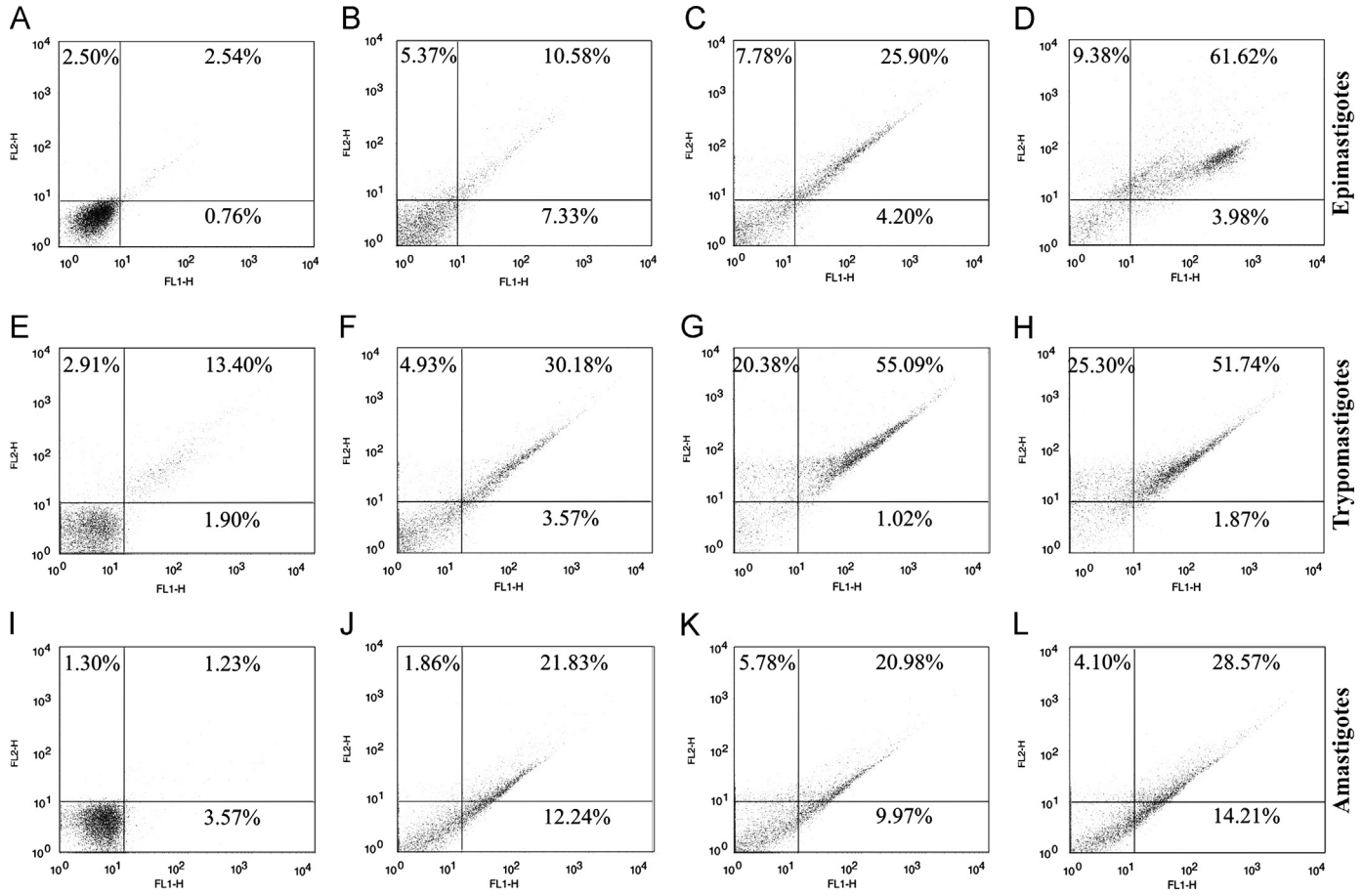

Fig. 9. Phosphatidylserine exposure in parasitic forms of *T. cruzi* treated with eupomatenoid-5 for 3 h using annexin-V FITC and PI. (A) Untreated epimastigotes. (B, C, D) Epimastigotes treated with 23.8, 51.0, and 170.0 μM. (E) Untreated trypomastigotes. (F, G, H) Trypomastigotes treated with 34.0, 68.0, and 170.0 μM. (I) Untreated amastigotes. (J, K, L) Amastigotes treated with 34.0, 68.0, and 170.0 μM. Percentage of annexin-V-stained positive cells is shown in the upper and lower right quadrants. Typical histograms of at least three independent experiments are depicted.

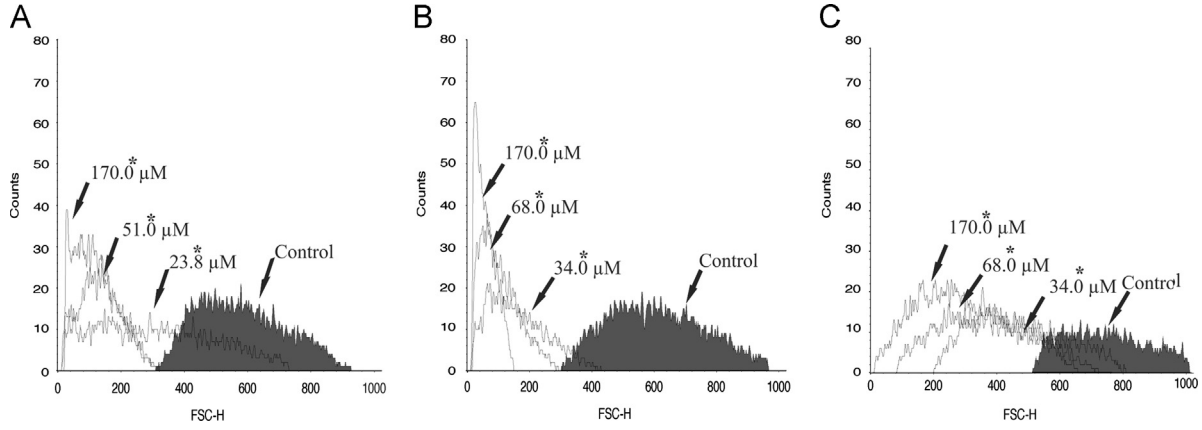

Fig. 10. Cell volume in parasitic forms of *T. cruzi* treated with eupomatenoid-5 for 3 h. (A) Epimastigotes treated with 23.8, 51.0, and 170.0 μM. (B) Trypomastigotes treated with 34.0, 68.0, and 170.0 μM. (C) Amastigotes treated with 34.0, 68.0, and 170.0 μM. FSC-H was considered as a function of cell size. Arrows correspond to concentrations tested. Control group (untreated cells) is also shown. Typical histograms of at least three independent experiments are depicted. $^{*}p \leq 0.05$, significant difference relative to the control group (untreated cells).

assays, the three parasitic forms, especially trypomastigotes (i.e., the infective and nonreplicative form of *T. cruzi*), exhibited marked reductions in $\Delta\Psi m$ and alterations in plasma membrane permeability. Trypomastigotes have a reduced $\Delta\Psi m$ as a result of remodeling during the life cycle of *T. cruzi* [31]. These data strongly suggest that any compound (e.g., eupomatenoid-5) with mitochondrion affinity can easily reduce $\Delta\Psi m$. In fact, increasingly more papers have been published that describe trypanocidal compounds that target *T. cruzi* mitochondria [24,32].

We showed that eupomatenoid-5 also induced oxidative imbalance in the three parasitic forms, reflected by an increase in ROS/RNS formation and decrease in the activity of TR, an enzyme that participates in the hydroperoxide detoxification of trypanosomatids through the trypanothione-dependent system [14].

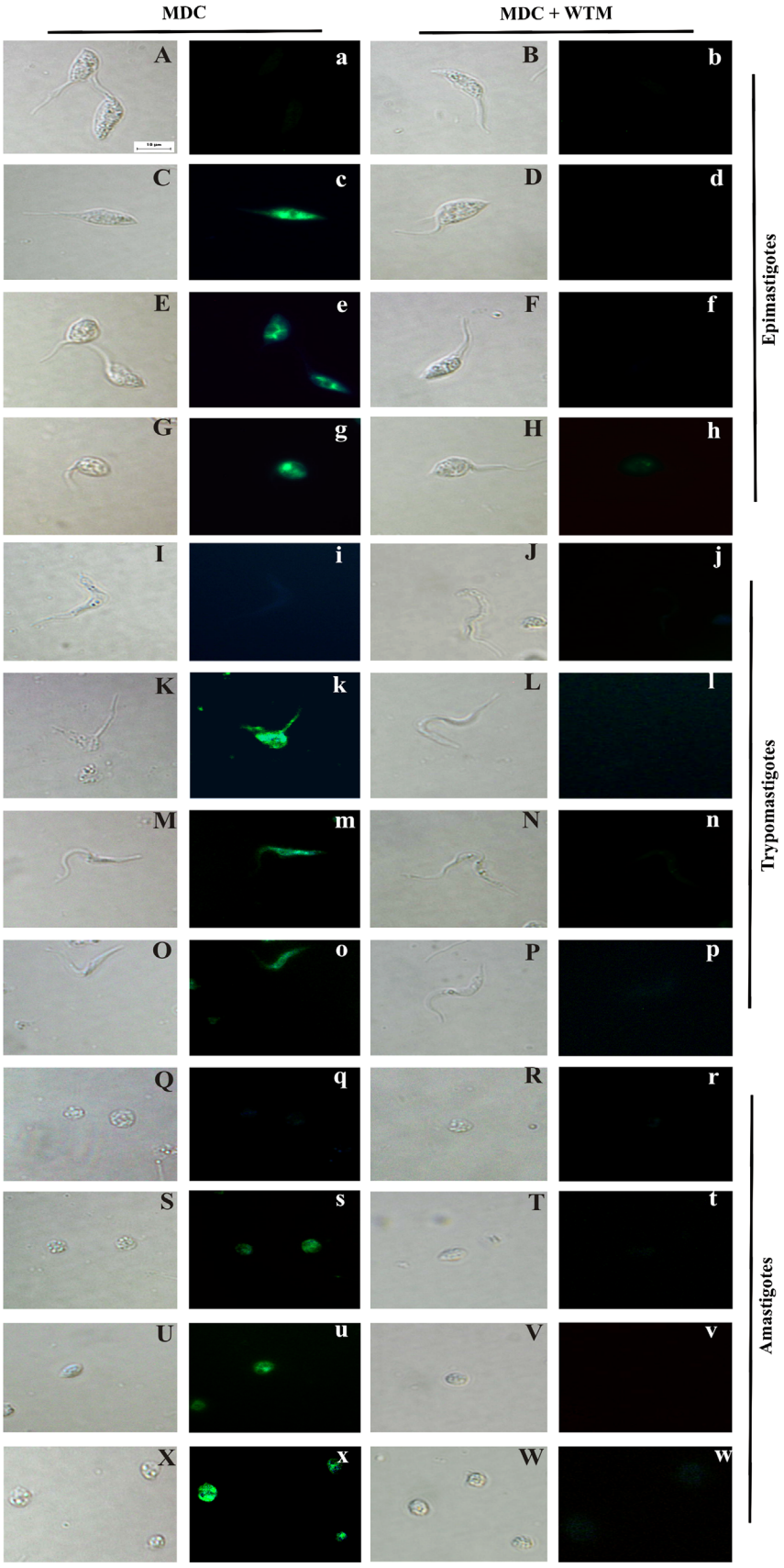

Fig. 11. Autophagic vacuoles in parasitic forms of *T. cruzi* treated with eupomatenoid-5 for 24 h using labeling with MDC, a fluorescent probe that accumulates in autophagic vacuoles. (A–X) DIC. (a–x) Fluorescence. (A, a, B, b) Untreated epimastigotes. (C, c, E, e, G, g) Epimastigotes treated with 23.8, 51.0, and 170.0 μM. (D, d, F, f, H, h) Epimastigotes treated with 23.8, 51.0, and 170.0 μM + 0.5 μM wortmannin (WTM). (I, i, J, j) Untreated trypomastigotes. (K, k, M, m, O, o) Trypomastigotes treated with 34.0, 68.0, and 170.0 μM. (L, l, N, n, P, p) Trypomastigotes treated with 34.0, 68.0, and 170.0 μM + 0.5 μM WTM. (Q, q, R, r) Untreated amastigotes. (S, s, U, u, X, x) Amastigotes treated with 34.0, 68.0, and 170.0 μM. (T, t, V, v, W, w) Amastigotes treated with 34.0, 68.0, and 170.0 μM + 0.5 μM WTM. The images are representative of treated epimastigotes, trypomastigotes, and amastigotes of at least three independent experiments. Scale bar, 10 μm.

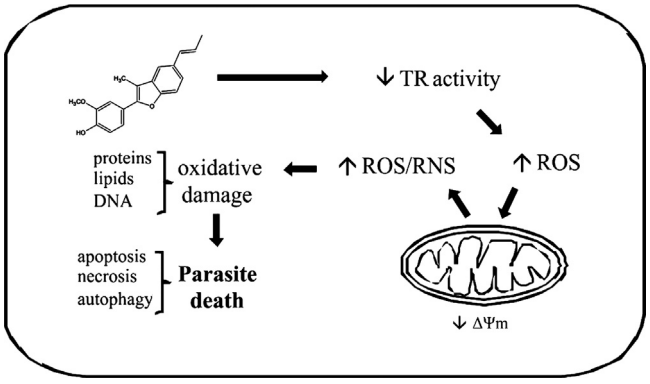

Fig. 12. Mechanistic assumptions about the trypanocidal action of eupomatenoid-5. Eupomatenoid-5 decreases TR activity, leading to a relative increase in ROS that triggers mitochondrial depolarization (loss of $\Delta\Psi m$) followed by an absolute increase in mitochondrial ROS/RNS production through the electron transport chain. This increase in ROS/RNS induces oxidative damage, leading to parasite death.

Oxidative stress was then observed, reflected by lipid peroxidation and DNA fragmentation. Surprisingly, these alterations were more pronounced in trypomastigotes, which exhibit increased levels of antioxidant enzymes and should more efficiently detoxify than the other forms [14,31]. In fact, trypanocidal compounds have been shown to target enzymes involved in the peroxide detoxification of *T. cruzi* [33,34].

In this context, two questions arise. What came first, the decrease in antioxidant enzyme activity or the increase in ROS/RNS? Should the increase in ROS/RNS formation induced by eupomatenoid-5 be considered a cause or a consequence of mitochondrial dysfunction? The increase in ROS/RNS formation might occur in mitochondria. In addition to the synthesis of adenosine triphosphate, mitochondria are also involved in the formation of ROS/RNS [35]. Mitochondrial ROS/RNS formation is essential in many signaling processes and strongly involved in the degenerative process through damage to macromolecules, mainly proteins, lipids, and DNA [31,36–38]. However, the increase in ROS/RNS might also involve antioxidant enzyme impairment. Our thiol, DHR, MitoSOX, and Rh123 data give us support to answer these questions. Eupomatenoid-5 decreased TR activity and increased ROS/RNS formation as soon as treatment began. In contrast, eupomatenoid-5 induced mitochondrial membrane depolarization only after 3 h treatment, which was observed in the Rh123 and DHR assays. Our overall hypothesis is that the mechanism of action of eupomatenoid-5 involves a decrease in hydroperoxide detoxification by reducing TR activity, leading to a relative increase in ROS that triggers mitochondrial depolarization, followed by an absolute increase in mitochondrial ROS/RNS production through the electron transport chain (Fig. 12). This increase in ROS/RNS then acts in any membrane of the parasite, including the mitochondrial membrane, further impairing mitochondrial function and possibly inducing more ROS/RNS generation [39,40]. This scenario made us believe that the increase in ROS/RNS is both a cause and a consequence of mitochondrial dysfunction. This phenomenon is conceivable and well supported by the ROS-induced ROS-release process [41].

The experiments presented herein provide evidence that eupomatenoid-5 induced biochemical and morphological alterations in *T. cruzi*, leading to parasite death. Based on the present DNA fragmentation, phosphatidylserine exposure, and reduced parasite volume data, we strongly believe that apoptosis is a cell death pathway involved in the trypanocidal action of eupomatenoid-5. Based on plasma membrane disruption, necrosis could also be an alternative pathway of cell death induced by eupomatenoid-5. In addition to apoptosis and necrosis, the presence of autophagic vacuoles, revealed by MDC labeling, suggests autophagic death. All of these cell death pathways have been well described for trypanosomatids, with significant mitochondrion participation [20,42,43]. Classic ways in which these parasite mitochondria are involved in apoptosis, necrosis, and autophagy include a loss of membrane potential and increase in ROS formation [29,44,45]. Accumulating evidence suggests that a key event in the transition from apoptosis to necrosis or autophagy involves an excessive increase in mitochondrial ROS formation [40,44].

In conclusion, the present data provide further insights into the mechanisms of action of eupomatenoid-5. Additionally, our data strongly suggest that eupomatenoid-5 is an effective compound to treat Chagas disease, with remarkable trypanocidal action against the three main forms of *T. cruzi,* including trypomastigotes and amastigotes. Therefore, eupomatenoid-5 might be an effective compound for further in vivo analysis. Notably, our data indicate that the trypomastigote form is the most sensitive to the effects of eupomatenoid-5. Trypomastigotes are the only nonreplicative form of the *T. cruzi* life cycle. Metacyclogenesis, the process by which the various forms of *T. cruzi* are transformed from noninfectious and replicative into infectious and nonproliferative, remains unclear. The literature provides information only about changes in the pattern of gene expression [46,47]. Therefore, our hypothesis is that eupomatenoid-5 might take advantage of this process and have more efficient actions against trypomastigote forms of *T. cruzi*. Actually, drug resistance is well known for the various strains of *T. cruzi* because this parasite is a heterogeneous group with morphological, physiological, biochemical, and clinical diversity [48].

Acknowledgments

This work was supported through grants from the Conselho Nacional de Desenvolvimento Científico e Tecnológico, Capacitação de Aperfeiçoamento de Pessoal de Nível Superior, Financiadora de Estudos e Projetos, PRONEX/Fundação Araucária, Programa de Pós-Graduação em Ciências Farmacêuticas da Universidade Estadual de Maringá, and Complexo de Centrais de Apoio a Pesquisa–UEM.

References

[1] Andreollo, N. A.; Malafaia, O. Os 100 anos da doença de Chagas no Brasil. *ABCD Arq. Bras. Cir. Dig* **22:**189–191; 2009.
[2] World Health Organization *First WHO report on neglected tropical diseases: working to overcome the global impact of neglected tropical diseases*. Geneva: WHO; 2010. 1–172.
[3] Caballero, A. P.; Marín, C.; Rodríguez-Diéguez, A.; Ramírez-Macíaz, I.; Barea, E.; Sánchez-Moreno, M.; Salas, J. M. *In vitro* and *in vivo* antiparasital activity against *Trypanosoma cruzi* of three novel 5-methyl-1,2,4-triazolo[1,5-*a*]pyrimidin-7(4H)-one-based complexes. *J. Inorg. Biochem.* **105:**770–776; 2011.
[4] Chagas, C. Nova tripanossomíase humana: estudos sobre a morfologia e o ciclo evolutivo do *Schizotrypanum cruzi* n. gen., n. sp., agente etiológico de nova entidade mórbida do homem. *Mem. Inst. Oswaldo Cruz* **1:**159–218; 1909.
[5] Brener, Z. Present status of chemotherapy and chemoprophylaxis of human trypanosomiasis in the Western Hemisphere. *Pharm. Ther* **7:**71–90; 1979.
[6] Izumi, E.; Ueda-Nakamura, T.; Dias Filho, B. P.; Veiga Júnior, V. F.; Nakamura, C. V. Natural products and Chagas' disease: a review of plant compounds studied for activity against *Trypanosoma cruzi*. *Nat. Prod. Rep.* **28:**809–823; 2011.
[7] Veiga-Santos, P.; Pelizzaro-Rocha, K. J.; Santos, A. O.; Ueda-Nakamura, T.; Dias Filho, B. P.; Silva, S. O.; Sudatti, D. B.; Bianco, E. M.; Pereira, R. C.; Nakamura, C. V. *In vitro* anti-trypanosomal activity of elatol isolated from red seaweed *Laurencia dendroidea*. *Parasitology* **137:**1661–1670; 2010.
[8] Menna-Barreto, R. F. S.; Laranja, G. A. T.; Silva, M. C. C.; Coelho, M. G. P.; Paes, M. C.; Oliveira, M. M.; Castro, S. L. Anti-*Trypanosoma cruzi* activity of *Pterodon pubescens* sees oil: geranylgeraniol as the major bioactive component. *Parasitol. Res.* **103:**111–117; 2008.
[9] Kollien, A.; Schaub, G. The development of *Trypanosoma cruzi* in Triatominae. *Parasitol. Today* **16:**381–387; 2000.
[10] Maya, J. D.; Cassels, B. K.; Iturriaga-Vásquez, P.; Ferreira, J.; Faúndez, M.; Galanti, N.; Ferreira, A.; Morello, A. Mode of action of natural and synthetic

drugs against *Trypanosoma cruzi* and their interaction with the mammalian host. *Comp. Biochem. Physiol* **146:**601–620; 2007.
[11] Luize, P. S.; Ueda-Nakamura, T.; Dias-Filho, B. P.; Cortez, D. A. G.; Nakamura, C. V. Activity of neolignans isolated from *Piper regnellii* (MIQ.) C.DC. var. *pallescens* (C.DC.) YUNCK against *Trypanosoma cruzi*. *Biol. Pharm. Bull.* **10:**2126–2130; 2006.
[12] Luize, P. S.; Ueda-Nakamura, T.; Dias-Filho, B. P.; Cortez, D. A. G.; Morgado-Diaz, J. A.; De Souza, W.; Nakamura, C. V. Ultrastructural alterations induced by the neolignan dihydrobenzofuranic eupomatenoid-5 on epimastigote and amastigote forms of *Trypanosoma cruzi*. *Parasitol. Res.* **100:**31–37; 2006.
[13] Pelizzaro-Rocha, K. J; Veiga-Santos, P.; Lazarin-Bidóia, D.; Ueda-Nakamura, T.; Dias Filho, B. P.; Ximenes, V. F.; Silva, S. O.; Nakamura, C. V. Trypanocidal action of eupomatenoid-5 is related to mitochondrion dysfunction and oxidative damage in *Trypanosoma cruzi*. *Microbes Infect.* **13:**1018–1024; 2011.
[14] Irigoín, F.; Cibils, L.; Comini, M. A.; Wilkinson, S. R.; Flohe, L.; Radi, R. Insights into the redox biology of *Trypanosoma cruzi:* trypanothione metabolism and oxidant detoxification. *Free Radic. Biol. Med.* **45:**733–742; 2008.
[15] Chauret, D. C; Bernad, C. B.; Arnason, J. T.; Durst, T. Insecticidal neolignans from *Piper decurrens*. *J. Nat. Prod.* **59:**152–155; 1996.
[16] Camargo, E. P. Growth and differentiation in *Trypanosoma cruzi:* origin of metacyclic trypanosomes in liquid media. *Rev. Inst. Med. Trop. São Paulo* **6:**93–100; 1964.
[17] Boiani, M.; Piacenza, L.; Hernández, P.; Boiani, L.; Cerecetto, H.; González, M.; Denicola, A. Mode of action of Nifurtimox and *N*-oxide-containing heterocycles against *Trypanosoma cruzi:* is oxidative stress involved? *Biochem. Pharmacol.* **79:**1736–1745; 2010.
[18] Shukla, A. K.; Patra, S.; Dubey, V. K. Iridoid glucosides from *Nyctanthes arbortristis* result in increased reactive oxygen species and cellular redox homeostasis imbalance in Leishmania parasite. *Eur. J. Med. Chem.* **54:**49–58; 2012.
[19] Pompella, A.; Maellaro, E.; Casini, A. F.; Ferrali, M.; Ciccoli, L.; Comporti, M. Measurement of lipid peroxidation *in vivo:* a comparison of different procedures. *Lipids* **22:**206–211; 1987.
[20] Jimenez, V.; Paredes, R.; Sosa, M. A.; Galanti, N. Natural programmed cell death in *T. cruzi* epimastigotes maintained in axenic cultures. *J. Cell. Biochem.* **105:**688–698; 2008.
[21] Munafo, D. B.; Colombo, M. I. A novel assay to study autophagy: regulation of autophagosome vacuole size by amino acid deprivation. *J. Cell Sci.* **114:**3619–3629; 2001.
[22] Biederbick, A.; Kern, H. F.; Elsasser, H. P. Monodansylcadaverine (MDC) is a specific *in vivo* marker for autophagic vacuoles. *Eur. J. Cell. Biol.* **66:**3–14; 1995.
[23] Blommaart, E. F.; Krause, U.; Schellens, J. P.; Vreeling-Sindelárová, H.; Meijer, A. J. The phosphatidylinositol 3-kinase inhibitors wortmannin and LY294002 inhibit autophagy in isolated rat hepatocytes. *Eur. J. Biochem.* **243:**240–246; 1997.
[24] Menna-Barreto, R. F. S.; Gonçalves, R. S. L.; Costa, E. M.; Silva, R. S. F.; Pinto, A. V.; Oliveira, M. F.; Castro, S. L. The effect on *Trypanosoma cruzi* of novel synthetic naphthoquinones is mediated by mitochondrial dysfunction. *Free Radic. Biol. Med.* **47:**644–653; 2009.
[25] Leal, C. A.; Shetinger, M. R.; Leal, D. B.; Morsch, V. M.; Da Silva, A. S.; Rezer, J. F.; De Barros, A. V.; Jaques, J. A. Oxidative stress and antioxidant defenses in pregnant women. *Redox Rep.* **16:**230–236; 2011.
[26] Lima, E. S.; Abdalla, D. S. P. Peroxidação lipídica: mecanismos e avaliação em amostras biológicas. *Rev. Bras. Cien. Farm* **37:**293–303; 2001.
[27] Ba, X.; Gupta, D.; Davidson, M.; Garg, N. J. *Trypanosoma cruzi* induces the reactive oxygen species–PARP-1-RelA pathway for up-regulation of cytokine expression in cardiomyocytes. *J. Biol. Chem* **285:**11596–11606; 2010.
[28] Kosec, G.; Alvarez, V. E.; Agüero, F.; Sánchez, D.; Dolinar, M.; Turk, B.; Turk, V.; Cazzulo, J. J. Metacaspases of *Trypanosoma cruzi:* possible candidates for programmed cell death mediators. *Mol. Biochem. Parasitol.* **145:**18–28; 2006.
[29] Kroemer, G.; Galluzzi, L.; Vandenabeele, P.; Abrams, J.; Alnemri, E. S.; Baehrecke, E. H.; Blagosklonny, M. V.; El-Deiry, W. S.; Golstein, P.; Green, D. R.; Hengartner, M.; Knight, R. A.; Kumar, S.; Lipton, S. A.; Malorni, W.; Nuñez, G.; Peter, M. E.; Tschopp, J.; Yuan, J.; Piacentini, M.; Zhivotovsky, B.; Melino, G. Classification of cell death recommendations of the Nomenclature Committee on Cell Death. *Cell Death Differ.* **16:**3–11; 2009.
[30] Valdez, R. H.; Tonin, L. T. D.; Ueda-Nakamura, T.; Dias Filho, B. P.; Díaz, J. A. M.; Sarragiotto, M. H.; Nakamura, C. V. Biological activity of 1,2,3,4-tetrahydro-β-carboline-3-carboxamides against *Trypanosoma cruzi*. *Acta Trop.* **110:**7–14; 2009.
[31] Gonçalves, R. L. S.; Menna-Barreto, R. F. S.; Polycarpo, C. R.; Gadelha, F. R.; Castro, S. L.; Oliveira, M. F. A comparative assessment of mitochondrial function in epimastigotes and bloodstream trypomastigotes of *Trypanosoma cruzi*. *J. Bioenerg. Biomembr.* **43:**651–661; 2011.
[32] Fernandes, M. P.; Inada, N. M.; Chiaratti, M. R.; Araújo, F. F. B.; Meirelles, F. V.; Correia, M. T. S.; Coelho, L. C. B. B.; Alves, M. J. M.; Gadelha, F. R.; Vercesi, A. E. Mechanism of *Trypanosoma cruzi* death induced by *Cratylia mollis* seed lectin. *J. Bioenerg. Biomembr.* **42:**69–78; 2010.
[33] Giulivi, C.; Turrens, J. F.; Boveris, A. Chemiluminescence enhancement by trypanocidal drugs and by inhibitors of antioxidant enzymes in *Trypanosoma cruzi*. *Mol. Biochem. Parasitol.* **30:**243–252; 1988.
[34] Li, Z.; Fennie, M. W.; Ganem, B.; Hancock, M. T.; Kobaslija, M.; Rattendi, D.; Bacchi, C. J.; O'Sullivan, M. C. Polyamines with *N*-(3-phenylpropyl) substituents are effective competitive inhibitors of trypanothione reductase and trypanocidal agents. *Bioorg. Med. Chem. Lett.* **11:**251–254; 2001.
[35] Murphy, M. P. How mitochondria produce reactive oxygen species. *Biochem. J.* **417:**1–13; 2009.
[36] Kowaltowski, A. J.; Souza-Pinto, N. C.; Castilho, R. F.; Vercesi, A. E. Mitochondria and reactive oxygen species. *Free Radic. Biol. Med.* **47:**333–343; 2009.
[37] Smirlis, D.; Duszenko, M.; Jiménez-Ruiz, A.; Scoulica, E.; Bastien, P.; Fasel, N.; Soteriadou, K. Targeting essential pathways in trypanosomatids gives insights into protozoan mechanisms of cell death. *Parasit. Vectors* **3:**1–15; 2010.
[38] Fonseca-Silva, F.; Inacio, J. D. F.; Canto-Cavalheiro, M. M.; Almeida-Amaral, E. E. Reactive oxygen species production and mitochondrial dysfunction contribute to quercetin induced death in *Leishmania amazonensis*. *PLoS One* **6:**1–7; 2011.
[39] Rhoads, D. M.; Umbach, A. L.; Subbaiah, C. C.; Siedow, J. N. Mitochondrial reactive oxygen species: contribution to oxidative stress and interorganellar signaling. *Plant. Physiol.* **141:**357–366; 2006.
[40] Gupta, S.; Bhatia, V.; Wen, J. J.; Wu, Y.; Huang, M. H.; Garg, N. J. *Trypanosoma cruzi* infection disturbs mitochondrial membrane potential and ROS production rate in cardiomyocytes. *Free Radic. Biol. Med.* **47:**1414–1421; 2009.
[41] Zoro, D. B.; Filburn, C. R.; Klotz, L. O.; Zweier, J. L.; Sollott, S J. Reactive oxygen species (ROS)-induced ROS release: a new phenomenon accompanying the mitochondrial permeability transition in cardiac myocytes. *J. Exp. Med.* **192:**1001–1014; 2000.
[42] Menna-Barreto, R. F. S.; Salomão, K.; Dantas, A. P.; Santa-Rita, R. M.; Soares, M. J.; Barbosa, H. S.; Castro, S. L. Different cell death pathways induced by drugs in *Trypanosoma cruzi:* an ultrastructural study. *Micron* **40:**157–168; 2009.
[43] Kiel, J. A. K. W. Autophagy in unicellular eukaryotes. *Philos. Trans. R. Soc. B* **365:**819–830; 2010.
[44] Addabbo, F.; Montagnani, M.; Goligorsky, M. S. Mitochondria and reactive oxygen species. *Hypertension* **53:**885–892; 2009.
[45] Souza, E. M. Nefertiti, A. S. G.; Bailly, C.; Lansiaux, A.; Soeiro, M. N. C. Differential apoptosis-like cell death in amastigote and trypomastigote forms from *Trypanosoma cruzi*-infected heart cells *in vitro*. *Cell Tissue Res.* **341:**173–180; 2010.
[46] Krieger, M. A.; Ávila, A. R.; Ogatta, S. F. Y.; Plazanet-Menut, C.; Goldenberg, S. Differential gene expression during *Trypanosoma cruzi* metacyclogenesis. *Mem. Inst. Oswaldo Cruz* **94:**165–168; 1999.
[47] Cardoso, J.; Lima, C. P.; Leal, T.; Gradia, D. F.; Fragoso, S. P.; Goldenberg, S.; Sá, R. G.; Krieger, M. A. Analysis of proteasomal proteolysis during the *in vitro* metacyclogenesis of *Trypanosoma cruzi*. *PLoS One* **6:**e21027; 2011.
[48] Camandaroba, E. L. P.; Reis, E. A. G.; Gonçalves, M. S.; Reis, M. G.; Andrade, S. G. *Trypanosoma cruzi*: susceptibility to chemotherapy with benznidazole of clones isolated from the highly resistant Colombian strain. *Rev. Soc. Bras. Med. Trop.* **36:**201–209; 2003.